Umudike Journal of Engineering and Technology (UJET); Vol. 6, No. 1, June 2020, pp. 32 – 39; Michael Okpara University of Agriculture, Umudike, Print ISSN: 2536-7404, Electronic ISSN:2545-5257; http://ujetmouau.net; doi: https://doi.org/10.33922/j.ujet_v6i1_3



EFFECT OF CARBON PARTICULATE ON THE REACTIVITY OF ε-CAPROLACTAM IN IN SITU POLYMERISATION OF PA6/CARBON COMPOSITES

¹Umar M., ²Ofem M. I., ¹Anwar A. S. and ³Ubi P. A.

¹Department of Chemical Engineering, Kaduna Polytechnic, Kaduna Nigeria ²Department of Mechanical Engineering, Cross River University of Technology Calabar, Nigeria ³Department of Mechanical Engineering, University of Calabar, Nigeria

ABSTRACT

The effect of particulate carbon fillers, graphite (G) and Graphite nanoplatelet to the polymerisation reaction of epsilon caprolactam (EC) with a catalyst system consisting of N-acetyl caprolactam (NAC) and caprolactam magnesium bromide (CMB) was investigated. Two processing regimes were used each with 5 carbon cumulative loading levels. These are the 40/10 and 20/20 processing regimes where the first number reflect the percentage of sonication amplitude used and the next reflects the sonication time. The effects on polymerisation reaction rates and the properties of the composites were found to differ. For the G 40/10 system the rates of reaction for the composites are significantly reduced comparative to unfilled PA6. The rates of reaction fell from 0.3 to 0.15°C/s for the composites. For the G 20/20 system the rates of reaction fell within the range 0.3 ± 0.07 °C/s with error bars overlapping pure PA6. This suggests that relative to unfilled PA6 the dispersive mixing of G within the systems with the 20/20 dispersion condition had no significant effect on the rates of reaction.

Keywords: Graphite, nano-platelets, in situ polymerisation, melt extrusion, air, nitrogen, processing strain, rates of reaction, sonification

1. Introduction

The anionic polymerisation of the monomer ε-caprolactam (EC), to produce PA6 is typically initiated with a range of lactam-based activators and catalysts. The reaction's order and rate, kinetic rate constants, autocatalytic factors and activation energies are typically determined from experimental conversion/time [Van, et al., 2006, Greenley, et al., 1969, Mateva, et al., 1998], viscosity/time [Davé, et al., 1997, Penu, et al., 2011] or temperature/time [Davé, et al., 1997, Malkin, et al., 1982, Malkin, et al., 1979, Teuwen, et al., 2013, Horský, et al., 2003] data. In this study however, an approach is devised not to directly investigate the aforementioned rather, to study how under a quasi-adiabatic reaction condition, inclusion of graphitic particulates, synthetic graphite (G) and graphite nanoplatelets (GNP), their loading levels as well as their extent of dispersion affect the rates of polymerisation reactions.

While polymerisation reaction is taking place, the presence of any foreign particle is expected to interfere with the rates relative to the extent of its interaction which in turn, is expected to be influenced by size scale. At molecular scale, the presence of micron sized G particle and the nanosized

GNP, will influence the polymerisation rates anticipatively differently. Ordinarily, for pure PA6 polymerisation, when the same initial amounts of EC are used and polymerisation is conducted with equivalent catalysing species and initiated under similar conditions then, the reaction rates are expected to be identical. On this premise, when polymerisation with fillers is conducted, then, their loading level and size scale can favourably be ascribed the observed variations in the reactions rates.

2. Experimental Methodology

2.1. Materials and method

Caprolactam (C₆H₁₁NO, coded as EC) was purchased from Sigma-Aldrich, with purity level of 99 % and a molecular weight of 113.16. Pristine PA6, and EC were vacuum dried overnight at 50°C before usage which adequately rid of moisture. Methyl Magnesium Bromide (coded as MMB, molecular weight 119.26,) is a Grignard catalyst precursor which forms the catalyst, (Caprolactam Magnesium Bromide (CMB)) *in-situ*, was purchased Fisher Scientific as a 100 ml bottle containing a 3.0 M solution of MMB in diethyl ether. *Activator*: or co-catalyst, is a mono-functional N-acetylcaprolactam (C₈H₁₃NO₂, coded as NAC), supplied by Sigma-Aldrich with purity; 99 % and molecular weight of

155.19. *Graphite Filler*: Synthetic graphite, (coded as G) is ≤ 2 μ m in particle size was supplied by Sigma-Aldrich. *Graphite Nano-Platelets*: GNP-15, (coded as GNP) with surface area 107±7 m²/g, diameter of 15 μ m, aspect ratio of 1500 and density of 2 g/cm³ was bought from XG-Sciences, UK. Prior to use G and GNP are kept overnight in an oven at 160 °C.Pristine commercial grade PA6 was donated by Akulun Germany. The monomer Epsilon

2.2. Polymerisation Set-Up for PA6/Carbon Composites

The synthesis set-up (Fig 1) and a schematic diagram (Fig 2) are provided to assist in following the procedure. In Figure 1, the PA6/carbon composites polymerisation rig has two IKA overhead stirrers (labelled 1 & 2), a Cole Parmer sonication probe (3) and an IKA oil bath (4) set at 193±3°C. For blanketing, a dry N2 line (5) is provided. Using a temperature sensing device, a Pico-log (USB TC08) (6) interfaced to a lap-top computer (7), two k-type thermocouples (8 & 9) are logged to (7), one to record the temperature/time as the process progresses and the other to monitor the oil bath temperature. Two mixing components, stirring and sonication are simultaneously delivered (10). For the synthesis first and final stage, the stirrer is suspended above the oil bath as shown in (11).



Fig 1. PA6/Carbon Polymerisation set-up.

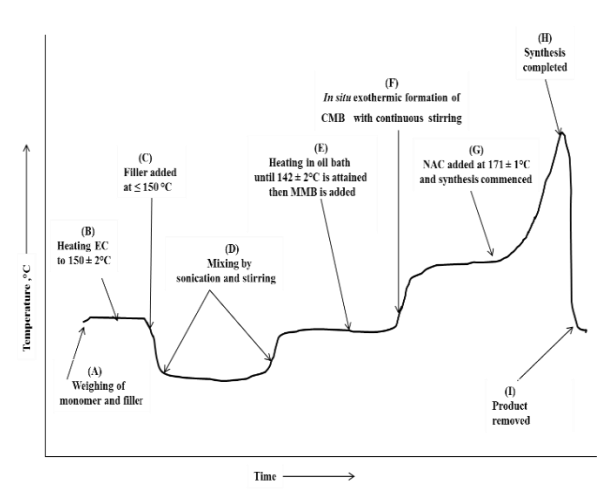


Fig. 2. Synthesis process description on a temperature/time line from A-I

2.3. Description of the PA6/Carbon Synthesis Stages

For both particulate carbons, the synthesis comprised of two separate systems. For systems designated as 40/10. sonication was at amplitude of 40 % for 10 min; whereas for systems designated as 20/20 the sonication was at 20 % amplitude for 20 min. Both systems passed through 3 synthesis stages represented in Figure 2 on a time line and in stages. In the first stage (A-C), the pre-weighed monomer (45g) was melted and allowed to attain 152 ±2 °C in the oil bath. Then, 0-25wt.% G at 5wt.% incremental intervals or GNP with 0-2.5wt.% loading, at 0.5wt.% incremental intervals is added. In stage ii (D), stirring began immediately at low speed. Within a minute, it was built-up to 2000 rpm. Then, the stirring was stepped down to 400 rpm to allow concurrent commencing of sonication. The last synthesis stage (E-I), the reaction vessel was returned to the oil bath, N₂ blanketing and thermocouple are inserted. Stirring begins at low speed and was increased within a minute to 2000 rpm. Using a micro-litre syringe, the required volume of the catalyst precursor. Methyl magnesium bromate was dispensed through the dry N₂ inlet at 142±2°C, (E). This leads to a sudden temperature rise due to the in-situ formation of the reaction catalyst, caprolactam magnesium bromide (CMB) while methane gas (F) guickly escapes through the open N2 inlet. The remnants of methane gas gradually escape through the loose thermocouple inlet. Equation 1 illustrates the reaction that took place.

$$CH_3 MgBr + (CH_2)_5 CONH \rightarrow (CH_2)_5 CONM_g Br + CH_4 \uparrow$$
 1

At point G the activator, NAC, is added through the N_2 inlet to activate polymerisation at $171\pm1^\circ$. The oil bath heating is turned off. At 180°C , stirring is stopped, the stirrer withdrawn, left suspended within the vessel but out of contact with the reacting mixture. As in [Keledi, *et al.*, 2012] N_2 supply is turned off just above 200°C . The vessel is removed from the oil bath once its temperature began to drop. After cooling, removal of crystallised and shrunk products occurred at point I with samples shown in Figure 3.



Fig. 3. Labelled PA6/carbon composite products.

3. Results and Discussion

In evaluating the reaction rates, assumption is made that the rate of crystallisation taking place alongside polymerisation has been significantly reduced. It has been reported [Wilfong, et al., 1992] that PA6 synthesis initiation temperatures above 145°C to minimise primary crystallisation occurring concurrently with polymerisation, while initiating PA6 polymerisation reaction at temperatures approaching 190°C suppresses primary crystallisation [Teuwen, et al., 2013]. To totally eliminate primary crystallisation. PA6 synthesis needs to occur above its crystalline melting temperature [Van, et al., 2006]. Given that relatively low concentrations of catalysing species were used, 170 °C was chosen as the synthesis temperature. This condition minimises the rate of primary crystallisation while adequately ensuring high reaction rates. maximum temperature rise attained after initiating the synthesis is due the combination of two exothermic activities. polymerisation reaction and primary crystallisation. Since both processes take simultaneously [Van, et al., 2006], separating them will be difficult. The rate of polymerisation ($\Delta T/\Delta t$) was estimated by simply dividing the magnitudes of time and temperature changes between the periods of commencing and completing the synthesis. Although the synthesis system is semi-adiabatic, in ideal adiabatic systems, the extent of reaction relates directly to temperature rise [Malkin, et al., 1982].

The reaction rate, kinetic order, kinetic rate constants, autocatalytic factors and activation energies for anionic polymerisation of ε-caprolactam to produce PA6 can be determined from experimental conversion and or time data [Van, et al., 2006, Greenley, et al., 1969, Mateva, et al., 1998], viscosity/time data [Davé, et al., 1997, Penu, et al., 2010] or temperature/time data [Davé, et al., 1997, Malkin, et al., 1982, Malkin, et al., 1979, Teuwen, et al., 2013, Horský, et al., 2003, Russo, et al., 2013]. However, in this research, an approach was devised not to directly investigate the mentioned kinetic parameters, but rather to study how the rate of reaction in a quasi-adiabatic system is affected by the presence of two particulate carbon fillers, G or GNP, their loading levels as well as their extent of dispersion. It is expected that these rates would be identical given that the synthesis was conducted with equivalent catalysing species, initiated at the same polymerisation temperature using the same initial amounts of the monomer, ε-caprolactam, (EC) [Udipi, et al., 1997, Ueda, et al., 1996]. Any variations observed in the rates of reactions compared to unfilled PA6 can be attributed to the presence of the carbon fillers. These reaction rates were estimated on the assumption that the rate of crystallisation taking place alongside the polymerisation has been significantly reduced. PA6 synthesis at temperatures above 145 °C has been shown to minimise primary crystallisation which takes place alongside polymerisation [Keledi, et al., 2012]. At 190 °C polymerisation temperature, the heat release and temperature rise due to crystallisation can be suppressed [Teuwen, et al., 2013] and totally eliminated by synthesizing above the crystalline melting temperature of PA6 [Wilfong, et al., 1992].

3.1 Reaction Rates

On the temperature versus time plot Figure 4, the sign of completing the synthesis corresponds with the point at which the trace begins to fall in gradient and the product begins to solidify. This indicates the completion of monomer conversion, the supressing of primary crystallisation and the beginning of secondary crystallisation [Horský, et al., 2004]. Therefore, in Figure 4, the sluggish temperature rise with time (onset indicated by arrow) is associated with exothermic heat releases due to secondary crystallisation and is excluded from the estimation of the rates.

There are effects on the rate of reaction due to reaction mixture/filler interactions which arise from the dispersive sonication and the distributive stirring of G and GNP in molten EC. In terms of the dispersive mixing [Hielscher, 2005], the key parameter is the energy imparted per unit volume (E/V). The energy imparted, E (Ws), is the product of the power output (P (W)) and the time of exposure (t (s)). As P is directly proportional to the amplitude of the probe, A (m), and in these systems the volume is constant, a constant value of the product A x t provides constant E/V. Thus, identical E/V values are provided by the conditions of 40 % amplitude of sonication for 10 min and by 20 % amplitude of sonication for 20 min that are imparted to the molten EC/carbon systems. Both increasing sonication power and time have being associated with increased carbon dispersion in EC [Hielscher, 2005]

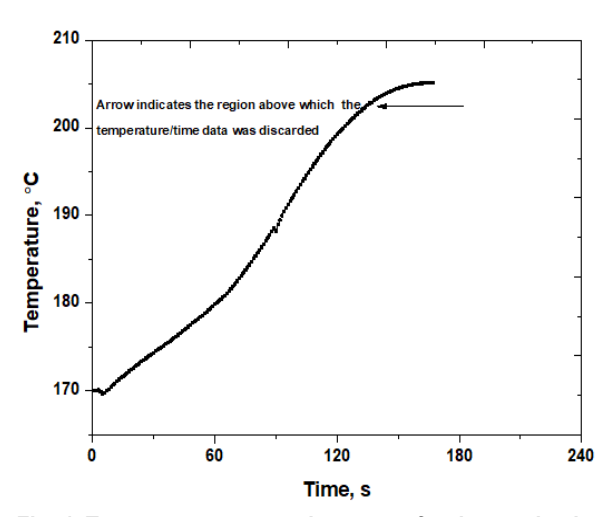


Fig. 4. Temperature versus time curve for the synthesis of PA 6/Carbon composites

3.2 Discussion on the G Based Reaction Rates

Figures 5 A and B suggest that the effect of graphite (G) on the two regimes G 40/10 and G 20/20 despite theoretically delivering equivalent power on the polymerising systems, are not the same on the rates of polymerisation. For the G 40/10 system (figure 5-A), the rates of reaction for the composites are significantly reduced comparative to unfilled PA6, with average values dropping from approximately 0.3 to 0.15 ± 0.025 °C/s for the composites. In contrast, for the G 20/20 system (figure 5-B), all the rates of reaction for the composites have error bars that overlap with that of pure PA6. All the systems reactivity fell within the range 0.3 ± 0.07 °C/s. This suggests that relative to unfilled PA6 the dispersive mixing of G within the systems with the 20/20

dispersion condition had lesser effect on the rates of reaction.

The addition of G at cumulative loading levels and under different mixing regimes can affect the final viscosities and thermal transport of all the systems. In the G-reaction mixture, the interfacial area generated is expected to improve thermal transport [Mateva, et al., 1998, Horský et al., 1999, (Ed.), KMI, Nylon Plastics Handbook. 1995] within the system and also increase the viscosity of the molten monomer epsilon caprolactam (EC) whereas, loading levels approaching 25G wt. % are proposed to hinder the polymerisation progress [Keledi, et al., 2012]. Viscosity rises can be expected to disrupt the ability of the catalysing species to generate activated monomers and hence hinder their subsequent joining with the reaction activator N-acetyl growing centres. Therefore, reaction rates may be expected to slow down at higher G loading. This suggests that the effect of G on the polymerisation of EC will depend on the G loading level and its state of dispersion; in particular, any deagglomeration or fracture of the fillers during direct sonication [Penu, et al., 2010].

Sonication has been shown to fragment and disperse carbon particles in EC proportionate to the period of exposure [Weng, et al., 2004], despite the fact that pristine G particles have a great tendency to re-agglomerate due to π -π interactions between the platelets [Xu and Gao 2010]. Horsky et al [Horský, et al., 2004] anticipated a decrease in rate of reaction when G loading was stepped-up wisely from 5 to 20 wt % in EC prior to in-situ polymerisation. In their systems [Horský, et al., 1999], this was only achieved when the equivalent mole % of catalysing species used was increased from 0.7-1.2 mole % as the G loading [Horský et al., 1999] increased. In their work [Horský et al., 1999], a significant decrease in polymerisation half time occurred which, suggests that the increased rate of reaction is essentially due to the increase in the mole % of the catalysing species which would have rather reduced due to the deactivating effect of G. Chemically refined G powder was reported to have only a minimal effect on the reaction rate of EC [Horský, et al., 2004, Horský, et al., 1999, Taurozzi, et al., 2011]. But this contradicts the findings of another study[Mateva, et al., 1998] where, the loading level of G was limited to only 2wt. %. The findings of these previous studies [Mateva, et al., 1998, Horský, et al., 2004, Horský, et al., 1999, Taurozzi, et al., 2011] appear to contradict one another, but, it can generally be inferred that G loading and conceivably its average particle size play significant but yet diverging roles.

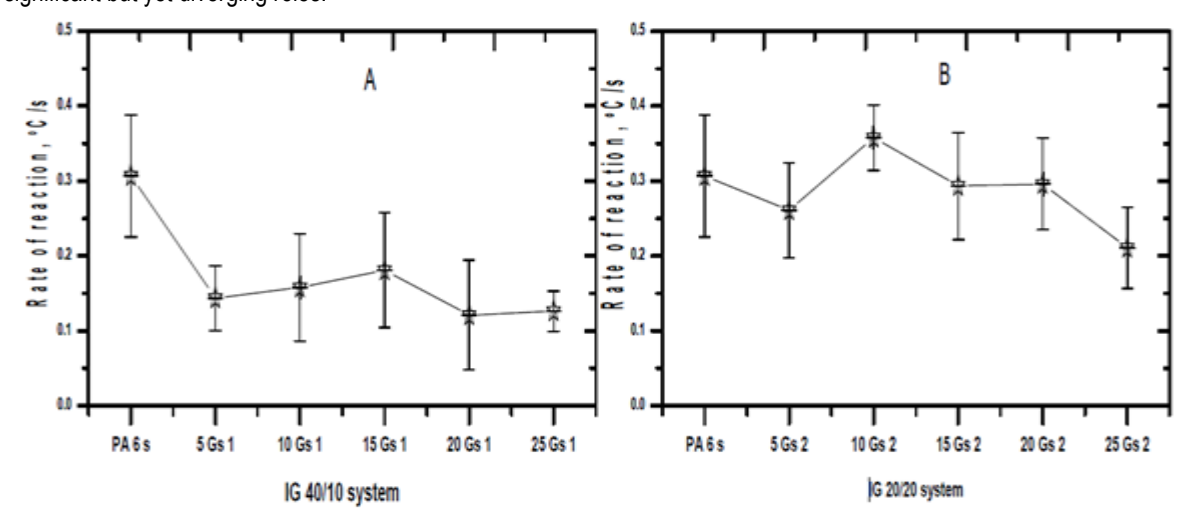


Fig. 5. Reaction rates for the G (graphite) based *in-situ* polymerisation systems: G 40/10 indicates 40% amplitude of sonication for 10 min and G 20/20 indicates 20% amplitude of for 20 min.

In this research, the two G systems, G 40/10 and G 20/20 were compared at equal values of E/V. But, at higher amplitudes of sonication, the rate of pressure fluctuation is greater [Hielscher, 2005, Taurozzi, et al., 2011] thereby causing more solid particles' breakages. G breaks relatively easily in-plane (exfoliation) the difference between the two systems may be the reflecting greater particle fracture in as shown in figure 5-A, causing greater reaction mixture/G interfacial surfaces with lower reaction rates compared to unfilled PA6 in the G 40/10 system. In the G20/20 (figure 5-B), where milder sonication amplitude is applied, the reaction rates maintained similar levels compared to the unfilled PA6. This suggests that there are fewer interfacial contacts between G and the reaction medium. Additionally, in the G 40/10 system where the dispersive sonication amplitude is higher, the reaction rates concurred more with that of [Horský, et al., 1999] where the average G particle used were 5 µm. The responses on reaction rates indicate inhibition thus suggesting that, the ability of G to hinder reaction progress increases with decreasing particle size but with the overall surface area increasing.

In both composite systems, a pattern of an increase in reaction rate to a peak value before a decline at higher G loading is observed. This pattern is more noticeable in the G 20/20 system. Considering the average values, the topmost average rate of reaction in the IG 20/20 system was attained not only at a lower G loading (10 Gs 2) but its average reaction rate of 0.36 °C/s doubled the highest of 0.18 °C/s

in the G 40/10 system (15 Gs 1). This suggests that the G dispersion and its subsequent interactions with the EC and the activating species in the reaction mixture are affected by the mixing regimes applied, which in turn influence the reaction rates. All equivalent composites (those with matching G loading) have higher reaction rates in the G 20/20 system than in the G 40/10 system. Moreover, 25Gs-2 which (considering average reaction rate values), has the lowest reaction rate in G 20/20 system equally has a reaction rate higher than 15Gs-1, the highest in the G 40/10 system.

If a particulate carbon filler such as G forms complexes with the catalysing species, then this complex is likely to depend on G loading, its dispersed state, its size and external exterior contours that result due to the mixing process [Penu, et al., 2010]. While ultrasonic power diminished the rate of polymerisation in an EC/CNT system [Xu and Gao 2010], the attendant dispersed state may be compensating [Penu, et al., 2011]. As such, it is proposed that, the mixing combination in G 40/10 has a higher fragmenting effect but a reduced carbon distribution compared to the G 20/20 system. As G particles fragment and disperse in the G 40/10 system, more reaction mixture-particle interface is created which led to a comparatively greater increase in viscosity compared to equivalent G loadings in the G 20/20 system. Therefore, the chance of generating particles with size scales significantly smaller than the micron-scale increased in the G 40/10 system. Since the stirring time in G 40/10 is just half that of its counterpart G 20/20 then, its G particles have greater tendency to re-agglomerate. Compared to unfilled PA6, the presence of fillers was proposed to have diverse effects on the anionic polymerisation of EC [Mateva, et al., 1998, Keledi, et al., 2012, Penu, et al., 2010, Horský, et al., 1999, Horský et al., 2001]. It was proposed that with viscosity rise due to filler addition in molten EC, activated monomers can be hindered from reaching active sites [Van, et al., 2006], whereas some filler surfaces deactivate catalysing species [Gong, et al., 2010]. For the G 40/10 system, it is proposed that the initial improvement in the average reaction rates which increases up to 15G wt. % may also be attributed to the fact that G particles may blanket the surface of EC against synthesis terminators such as H2O or air [Alford, et al., 2008]. Proton donors such as H₂O may deactivate catalyst on a one-to-one mole basis [Bogdanov, et al., 2000].

3.3 Discussion on the (Graphite Nanoplatelets) GNP Based Reaction Rates

Figure 6 (A & B) shows the reaction rates for the nanocomposite systems Nano platelets (GNP) NP 40/10 and NP 20/20 relative to unfilled PA6. In these systems, relative to EC, polymerisation began with 0.3 mole % each of the catalysing species. However, NP has a deactivating effect on the rate of reaction. Therefore, to ensure that the synthesis did not fail and equilibrium conversions remain attainable, the catalysing species mole % was stepped-up to 0.45 as from 1.5 NP wt. % loading. Notwithstanding, none of the reaction rate averages, matched that of the unfilled PA6 in both systems. In the NP 40/10 system (figure 6-A)

there are some overlaps in error bars between the unfilled PA6 and the nanocomposites; which clearly have lower reaction rates averages. All fell between 0.2-0.1, dropping from approximately 0.3 for the unfilled PA6. Among the nanocomposites, the reaction rates strongly overlapped. When equivalent catalysing species mole % is increased to 0.45, the rise and fall in the average reaction rates between 1.5NPs-1 and 2.0NPs-1 was likely induced by this dynamics. The average rate of reaction increased at 2.5NPs-1, overall rates remained within the limits of experimental error. This indicates that the extent of reaction inhibition created by the GNP depends on the level of interaction achieved between it and reacting species. This innately coincides with previous studies: where, when G enhanced the rate of polymerisation, the average particle size was 20 µm [Mateva, et al., 1998] and when it reduced same the average particle size was 5 µm [Horský et al., 1999]. Similarly, in the G 20/20 system, where a lesser fragmentation of the GNP was proposed to occur, some of the reaction rate averages were higher than that of the unfilled PA6. This further suggests that the inhibiting effect of GNP on the rate of reaction relates to its aspect ratio, interfacial area and size scale. Carbon nanotubes were found to inhibit reaction rates of EC [Penu, et al., 2010] but, at other instances, their residual metal catalyst were proposed to be reaction rate enhancers [Mateva, et al., 1998, Penu, et al., 2011]. Hence, similarity and size scale among particulate carbons is important since it affects the scale of mixing which in turn affects the rate of reaction.

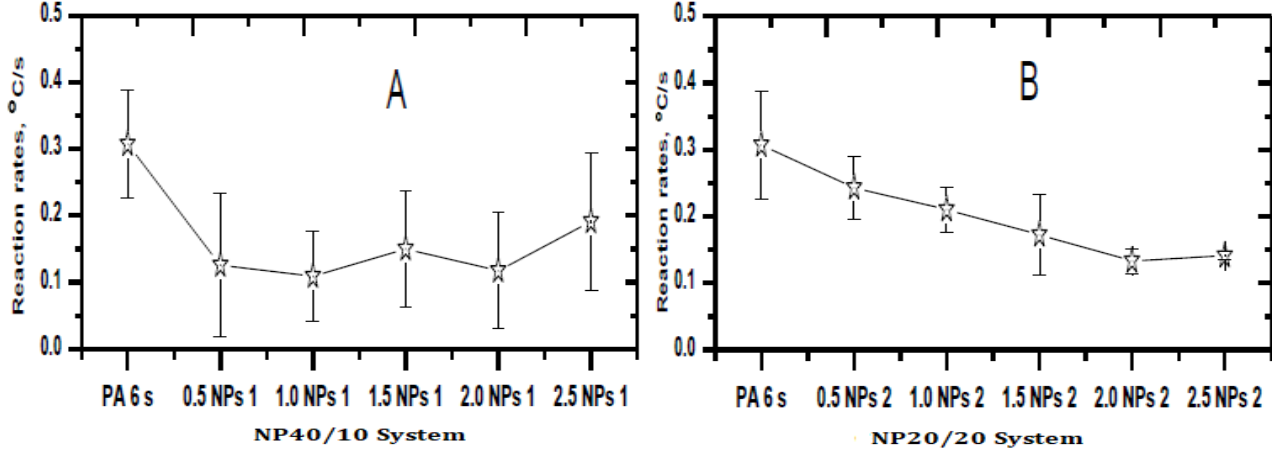


Fig. 6. The reaction rates for the NP *in situ* systems containing GNP. In A, GNP40/10 indicates 40% amplitude of sonication for 10 min. and GNP20/20 indicates 20% amplitude for 20 min.

Upon further reflections on the average rates of reaction as regards to the overlaps in standard deviation bars in NP

40/10 system, similarities are found with their micro-composite counterpart in the G 40/10 system. Both have

lower average reaction rates relative to the unfilled PA6. But when NP 40/10 is compared to NP 20/20 system, a reflection on the overall effects of the mixing delivered is brought into context. Regarding the average reaction rates in the NP 20/20 system figure 6 (B), a general reduction with increased GNP loading was seen. Initially, the reaction rates remained within the range of experimental error relative to the unfilled PA6 up to the intermediate loading level of 1.5 wt. %. Considering the average values, a linear reduction occurred up to 2.0 wt. % loading in spite of the accompanying 50 % increase in the mole % of the catalysing species. This provides better justification for the mid-way stepping up of the mole % of the catalysing species. Although sonication is less intense in the NP 20/20 system, the longer time spent, the simultaneous sonication and stirring appeared to cause more homogenous dispersion and distribution of the GNP particles.

In contrast, higher sonication amplitudes (even if only for half the exposure time) are more likely to cause particle fragmentation. Yet again, smaller particles have higher tendency to agglomerate. For the nano-scale thick GNP, this intensified particle-to-particle interaction [Wilfong, et al., 1992]. As a result, an overall better dispersed and less fragmented state for the GNP occurred in the NP 20/20 system. It is likely possible that, the 20/20 mixing regime rendered G and GNP particles in to a state where reaction rates are accelerated with the aid of complex formation between the catalyst and initiator [Van, et al., 2006].

4. Conclusion

The rates of polymerisation have been found to vary both with respect to mixing/dispersion, carbon type, loading and its size scale. The varied responses are not likely to be due to the presence of adsorbed impurities, or, in the case of GNP, the deactivating effect of minute residues of acid moieties because storing the carbon fillers at 160 °C has an annealing effect which volatilises remnants of acid moieties. Perhaps interaction between the carbon fillers and the catalysing species may lead to the formation of heavier and hence more sluggish complexes. Again, the possibility that side reactions occurred and interfered with the rates of reaction was minimised by initiating the synthesis at 170 °C which fell within a safe temperature regime. Irrespective of the loading the 20/20 systems were found to give higher reaction rates and this is proposed to be because carbon filler aspect ratios and external structures were better preserved due to and evenly dispersed with fewer

tendencies towards agglomeration. As a result, higher reaction rates were recorded for both the GNP and G. In some instance, the best in the 40/10 processing regime and only half as good as the least reactive in the 20/20 regime.

REFERENCES

Alford J. M., Bernal C., Cates M., and Diener M. D. (2008): Fullerene production in sooting flames from 1, 2, 3, 4-tetrahydronaphthalene. Carbon, Vol. 46, No.12, pp 1623-1625.

Bogdanov A., Deininger D., and Dyuzhev G. (2000): Development prospects of the commercial production of fullerenes. Technical Physics, Vol. 45, No.5 pp 521-527.

Davé R. S., Kruse R. L., Udipi K., and Williams D. E. (1997): Polyamides from lactams via anionic ring-opening polymerization: 3. Rheology. Polymer, Vol. 38, No.4, pp 949-954.

Davé R. S., Kruse R. L., Stebbins L. R., and Udipi K. (1997): Polyamides from lactams via anionic ring-opening polymerization: 2. Kinetics. Polymer, Vol. 38, No.4, pp 939-947.

Greenley R. Z., Stauffer J. C., and Kurz J. E. (1969): The Kinetic Equation for the Initiated, Anionic Polymerization of n-Caprolactam. Macromolecules, Vol. 2, No.6, pp 561-567.

Gong Y., Liu A., and Yang G. (2010): Polyamide single polymer composites prepared via in situ anionic polymerization of ϵ -caprolactam. Composites Part A: Applied Science and Manufacturing, Vol. 41, No.8, pp 1006-1011.

Hielscher T. E. (2005): Ultrasonic production of nano-size dispersions and emulsions. in ENS'05 Paris, France.

Horský J., Kolařík J., and Fambri L. (1999): Composites of alkaline poly(6-hexanelactam) with solid lubricants: one-step synthesis, structure, and mechanical properties. Die Angewandte Makromolekulare Chemie, Vol. 271, No.1, pp 75-83.

Horský J., Kolařík J., and Fambri L. (2003): One-Step Synthesis of Hybrid Composites of Poly(6-hexanelactam) Combining Solid Tribological Additives and Reinforcing Components. Macromolecular Materials and Engineering, Vol. 288, No.5, pp 421-431.

Horský J., Kolařík J., and Fambri L. (2004): Structure and Mechanical Properties of Composites of Poly (6-hexanelactam) Combining Solid Tribological Additives and

Reinforcing Components. Macromolecular Materials and Engineering, Vol. 289, No.4, pp 324-333.

Horský J., Kolařík J., and Fambri L. (1999): Composites of alkaline poly (6-caprolactam) and short glass fibers: one-step synthesis, structure and mechanical properties. Die Angewandte Makromolekulare Chemie, Vol. 264, No.1, pp 39-47

Horský J., Kolařík J., and Fambri L. (2001): Gradient Composites of Alkaline Poly (6-hexanelactam) with Graphite: One-Step Synthesis, Structure, and Mechanical Properties. Macromolecular Materials and Engineering, Vol. 286, No.4, pp 216-224

Keledi G., Hári J., and Pukánszky B. (2012): Polymer nanocomposites: structure, interaction, and functionality. Nanoscale, Vol. 4, No.6, pp 1919-1938.

KMI, Nylon Plastics Handbook. (1995): Munich Vienna New York: Hanser Publishers

Mateva R., Ishtinakova O., Nikolov R. N., and Djambova C. (1998): Kinetics of polymerization of ϵ -caprolactam in the presence of inorganic dispersed additives. European Polymer Journal, Vol. 34, No. 8, pp 1061-1067.

Malkin A. Y., Ivanova S. L., Frolov V. G., Ivanova A. N., and Andrianova Z. S. (1982): Kinetics of anionic polymerization of lactams.(Solution of non-isothermal kinetic problems by the inverse method). Polymer, Vol. 23, No. 12, pp 1791-1800.

Malkin A. Y., Frolov V. G., Ivanova A. N., and Andrianova Z. S. (1979): The nonisothermal anionic polymerization of caprolactam. Polymer Science USSR,; Vol. 21, No.3, pp 691-700.

Penu C., Hu G., Fonteix C., Marchal P., Choplin L., and Feng L. (2011): Effects of carbon nanotubes and their state of dispersion on the anionic polymerization of ϵ -caprolactam: II. Rheology. Polymer Engineering & Science, Vol. 51, No.6, pp 1116-1121.

Penu C., Hu G., Fonteix C., Marchal P., and Choplin L. (2010): Effects of carbon nanotubes and their state of dispersion on the anionic polymerization of ϵ -caprolactam: 1. Calorimetry. Polymer Engineering & Science, Vol. 50, No.12, pp 2287-2297.

Teuwen JJ, Geenen AA and Bersee HE (2013): Novel Reaction Kinetic Model for Anionic Polyamide-6. Macromolecular Materials and Engineering, Vol. 298, No. 2, pp 163-173..

Ricco L., Russo S., Orefice G., and Riva F (1999): Anionic poly (ϵ -caprolactam): Relationships among conditions of synthesis, chain regularity, reticular order, and polymorphism. Macromolecules, Vol. 32, No.23, pp 7726-7731.

Russo S, Maniscalco S, Moretti P and Ricco L (2013): Fast-activated anionic polymerization of ϵ - caprolactam in the bulk under quasi-adiabatic conditions: Comparison of different kinetic models. Journal of Polymer Science Part A: Polymer Chemistry Vol. 51, No.20, pp 4474-4480.

Taurozzi JS, Hackley VA and Wiesner MR (2011): Ultrasonic dispersion of nanoparticles for environmental, health and safety assessment-issues and recommendations. Nanotoxicology, Vol. 5, No.4, pp 711-729.

Udipi K, Davé RS, Kruse RL and Stebbins LR (1997): Polyamides from lactams via anionic ring-opening polymerization: 1. Chemistry and some recent findings. Polymer, Vol. 38, No.4, pp 927-38.

Ueda K, Yamada K, Nakai M, Matsuda T, Hosoda M and Tai K. (1996): Synthesis of high molecular weight nylon 6 by anionic polymerization of ϵ -caprolactam. Polymer Journal, Vol. 28, No.5, pp 446-51.

Weng W., Chen G., Wu D., Chen X., Lu J., and Wang P. (2004): Fabrication and characterization of nylon 6/foliated graphite electrically conducting nanocomposite. Journal of Polymer Science Part B: Polymer Physics, Vol. 42, No.15, pp 2844-2856

Wilfong D, Pommerening C and Gardlund Z (1992): Separation of polymerization and crystallization processes for nylon-6. Polymer, Vol. 33, No.18, pp 3884-3888.

Xu Z and Gao C (2010): In situ Polymerization Approach to Graphene-Reinforced Nylon-6 Composites. Macromolecules, Vol. 43, No.16, pp 6716-6723.

Van Rijswijk, K., Bersee H. E. N., Jager W. F., and Picken S. J. (2006): Optimisation of anionic polyamide-6 for vacuum infusion of thermoplastic composites: choice of activator and initiator. Composites Part A: Applied Science and Manufacturing, Vol. 37, No.6, pp 949-956.